The Incorporation of Static Field Solutions Into the Finite Difference Time Domain Algorithm

David B. Shorthouse and C. J. Railton, *Member, IEEE*

***Abstract*—This paper demonstrates how the accuracy, speed and flexibility of FDTD analysis may be improved for the modelling of MMIC structures. Correction factors, obtained from the known behavior of static fields close to discontinuities, may be incorporated into the algorithm for application in the regions of high field variation where errors would otherwise occur. Application is made to both enclosed and open microstrip structures.**

I. Introduction

THE Finite Difference Time Domain (FDTD) method is now well-known. It was first formulated by Yee [1] in the 1960's, and has been extensively applied to electromagnetic scattering and coupling problems, e.g. [2], and more recently to the analysis of planar microwave components, e.g. [3]. Traditionally these kinds of problems are done in the frequency domain using analytically heavy methods such as the Spectral Domain method [4]. However, with high performance computers becoming increasingly affordable, coupled with the need for analysis of microwave integrated circuits (MMIC's) having complex geometries and containing nonlinear components becoming ever more pressing, time domain techniques, in particular the FDTD method, are becoming of increasing importance.

At present, the fabrication technology available to designers of MMIC's can outstrip the ability of marketed CAD tools to accurately predict circuit performance. This is especially true where the circuits have a high component density, are used at high frequencies, or contain novel components which have complex, multilayered structures. In [5], Railton and McGeehan demonstrated how the basic FDTD method can be enhanced by, for example, the inclusion of modified finite difference equations to cater for thin dielectric layers and by the use of a non-uniform lattice arrangement. These enhancements have the effect of reducing the number of variables required by the model for a given prediction accuracy. This gives a marked reduction in computer run time or an improvement in model accuracy for the same number of nodes. This paper describes how the FDTD technique may be enhanced further by incorporating knowledge of the asymptotic field behavior around microstrip discontinuities into the algorithm. Microstrip discontinuities, namely corners and edges, are the building blocks of MMIC's. The resulting decrease in model running times, achieved in this contribution, indicates that it will soon be practical to use the FDTD technique for the CAD and analysis of realistically complex MMIC structures on an engineer's workstation.

Manuscript received August 20, 1991; revised November 15, 1991.

The authors are with the Department of Electrical and Electronic Engineering, University of Bristol, Queens Building, University Walk, Bristol, BS8 1TR, England.

IEEE Log Number 9106767.

II. The Basic FDTD Technique and Sources of Error

In the mid-1960's, Yee [1] introduced a new means of solving Maxwell's time dependent equations using finite-differences. With this approach, the continuous electromagnetic field in a finite volume of space is sampled at distinct points (or nodes) in a space-lattice, and at distinct equally spaced points in time. Yee produced difference equations, for non-dispersive, non-varying, isotropic media, that are finite difference analogues of the time dependent Maxwell's equations. The basic FDTD technique, and the difference equations which are used have been detailed many times in the literature. For brevity, a shorthand notation is used in this paper, as shown below for the E_x and H_y field component difference equations:

$$E_x^{t+dt} = E_x^t + \frac{\delta t}{\epsilon}\left(\frac{H_y^- - H_y)}{\delta z} + \frac{(H_z - H_z^-)}{\delta y}\right) \quad (1)$$

$$H_y^{t+dt} = H_y^t + \frac{\delta t}{\mu}\left(\frac{(E_z^+ - E_z)}{\delta x} + \frac{(E_x - E_x^+)}{\delta z}\right) \quad (2)$$

where F_q^- indicates that the F_q field component comes from the preceding cell in the q-direction, and F_q^+ indicates that the F_q field component comes from the next cell on. Fig. 1 shows the local arrangement of field components around a unit cell of the space lattice, highlighting the location of the E_x and H_y difference equation variables.

The localized nature of the FDTD algorithm can be seen, whereby the new value of a field component in the model depends only on its last value and on the values of some of the field components surrounding it. Thereby, all field phenomena can be modelled, as though stepping through time, by repeatedly implementing the difference equations on the field components throughout the model lattice. Hence field propagation and coupling that occur

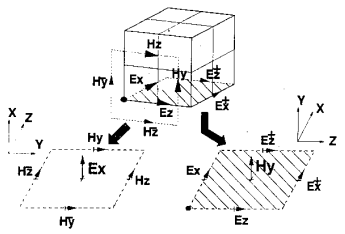

Fig. 1. Location of the *Ex* and *Hy* difference equation variables and a Yee unit cell.

on miniscule time and space scales may easily be investigated, e.g. [6].

Care must be taken to ensure that field resolution and stability considerations are met in deciding the configuration of the model. To ensure accuracy of field resolution and avoid ringing, any internodal distance, δ, must be a fraction of the minimum wavelength, $\lambda_{\min}$, expected in that region. It is found that reliable working constraints are ensuring that $\delta < \lambda_{\min}/20$ close to discontinuities, and $\delta < \lambda_{\min}/10$ elsewhere. In addition, to ensure model stability, the choice of time step, δt, is governed by

$$\delta t \leq \frac{1}{\nu_{\max}} \left(\frac{1}{\delta x^2} + \frac{1}{\delta y^2} + \frac{1}{\delta z^2} \right)^{-1/2} \tag{3}$$

as derived by Taflove and Brodwin [7]. Here, $\nu_{\max}$ is the maximum wave phase velocity expected, and the δx, δy, and δz are the smallest values for a cell in the model. This condition penalises the use of small internodal distances by insisting on a proportionally smaller time step, which necessitates more iterations for a model when cycling through a set time span.

To calculate frequency dependent parameters from the model, Fourier Transforms are performed on the time-domain data collected from specified nodes over the course of a run. Two main FDTD analysis techniques are commonly used; the resonator method for closed structures and the pulse excitation method for open structures. Firstly, the resonator method, as used by Choi and Hoefer [8], where the model is surrounded by electric walls, (simulated by ensuring that the tangential electric and normal magnetic field components on the walls are maintained at zero), and is given an initial excitation and left to oscillate. After an initial transient period, the model settles to its resonant steady-state. A time domain history is then taken, and a Fourier Transform search provides the frequencies of the resonant modes. This technique can also be used in conjunction with SDM [9] to calculate design parameters of the structure. Secondly, the pulse excitation method, as used by Reineix and Jecko [10], and by Zhang and Mei [11]. Here, the model is surrounded by absorbing boundaries, where applicable. A pulse is put onto a feed-line and allowed to propagate completely throughout the structure. The Fourier Transforms of the incident, transmitted and reflected waves are used to calculate the *S*-parameters of the structure. Both of these methods are used to give results in this contribution to demonstrate the generality of the modifications made to the FDTD method.

It is well-known, as demonstrated by De Smedt and Van Bladel in [12], that the perpendicular field components close to a perfectly conducting metallic strip edge, in the plane of the edge become singular as $r^{-0.5}$. The FDTD algorithm was formed through pointwise derivative approximations of Maxwell's equations, that assumes that all the field components behave linearly between nodes. Because the local truncation error of the FDTD approximation depends on the higher order derivatives of the field, it is to be expected that any inaccuracies in the FDTD analysis will most likely occur in the regions of high field variation that are found near discontinuities.

An analytically undemanding technique can be used to reduce inaccuracies by increasing the nodel density of the model. However, this is doubly costly in computer resources as it would both increase model nodes and hence variables, *and* decrease the iteration time step necessitating extra iterations. The original FDTD method has been enhanced to allow the use of a nonuniform lattice which enables the nodel density to be increased close to discontinuities, and decreased elsewhere. While this gives significant processing time and accuracy improvements over using a regular lattice, it still has time step penalties. A remedy to this problem was sought by introducing a different perspective into the FDTD algorithm.

III. Another Perspective

Taflove *et al.* [13] derived the basic FDTD difference equations starting from the integral forms of Ampere's law and Faraday's law. They demonstrated a limited 2-D modification of the FDTD algorithm close to discontinuities. Their insight is necessary in developing a full FDTD modification as it transforms our picture of the Yee lattice into a three dimensional chain-link array of intersecting orthogonal contours. This equivalent understanding of the model space helps to shed more light into the effect of microstrip discontinuities on the FDTD algorithm:

Ampere's Integral Law:

$$\frac{\partial}{\partial t} \int \varepsilon \boldsymbol{E} \cdot \boldsymbol{dS} = \oint \boldsymbol{H} \cdot \boldsymbol{dl} - \int \sigma \boldsymbol{E} \cdot \boldsymbol{dS} \tag{4}$$

Faraday's Integral Law:

$$\frac{\partial}{\partial t} \int \mu \boldsymbol{H} \cdot \boldsymbol{dS} = -\oint \boldsymbol{E} \cdot \boldsymbol{dl} \tag{5}$$

In forming the FDTD difference equations from the integral laws given above we make two forms of linear spatial approximation which are detailed below:

Surface Integral Approximation:

$$\int \mathbb{F} \cdot \boldsymbol{dS} \approx \hat{\mathbb{F}} \cdot \delta a \cdot \delta b \tag{6}$$

Line Integral Approximation:

$$\int \mathbb{F} \cdot \boldsymbol{dl} \approx \hat{\mathbb{F}} \cdot \delta l \tag{7}$$

where $\hat{\mathbb{F}}$ refers to the value of field, $\mathbb{F}$, that lies in the centre of each integral region, $\delta a\ \delta b$ is the area of the surface integral domain, and δl is the length of the line integral domain. It is obvious that these integral approximations become less accurate as the higher order spatial derivatives of the field, $\mathbb{F}$, show greater variation. This is most likely to happen around microstrip discontinuities where some fields are singular in nature. The H_y difference equation is now derived in brief to indicate where the above approximations feature in its formulation. Applying Faraday's law over the shaded region shown in Fig. 1, we obtain:

$$\frac{\partial}{\partial t}\int \mu \boldsymbol{H}_y \cdot \boldsymbol{dS} = -\oint \boldsymbol{E} \cdot \boldsymbol{dl}. \tag{8}$$

With linear approximations in space as in (6) and (7):

$$\frac{\partial}{\partial t}(\mu \cdot \hat{H}_y \cdot \delta x \cdot \delta z) = -(\hat{E}_x^+ - \hat{E}_x) \cdot \delta x + (\hat{E}_z - \hat{E}^+ z) \cdot \delta z). \tag{9}$$

With a linear approximation in time, we once again have the H_y difference equation:

$$H_y^{t+dt} = H_y^t \cdot \frac{\delta t}{\mu}\left(\frac{(E_z^+ - E_z)}{\delta x} + \frac{(E_x - E_x^+)}{\delta z}\right). \tag{10}$$

If we assume that the electromagnetic fields close to microstrip discontinuities assume their theoretical static forms, correction factors can be calculated for the integral approximations of the form of (6) and (7), as described from Section IV onwards. These correction factors can be used to form modified FDTD difference equations which can be applied at the nodes close to the discontinuities. Their values will depend on the detailed shape of the metal and the local lattice configuration. The correction factors are obtained by the direct evaluation of the above integral approximations using *a priori* knowledge of static field strengths and model geometry. The calculation is carried out prior to running the FDTD algorithm and contributes very little to the computational efforts required.

Hence, with the inclusion of correction factors CF_s and CF_1, approximations (6) and (7) become:

$$\int \mathbb{F} \cdot dS = \hat{\mathbb{F}} \cdot \delta a \cdot \delta b \cdot \mathrm{CF}_s \qquad \text{where } \mathrm{CF}_s = \frac{\int \mathbb{F} \cdot dS}{\hat{\mathbb{F}} \cdot \delta a \cdot \delta b} \tag{11}$$

$$\int \mathbb{F} \cdot dl = \hat{\mathbb{F}} \cdot \delta l \cdot \mathrm{CF}_1 \qquad \text{where } \mathrm{CF}_1 = \frac{\int \mathbb{F} \cdot dl}{\hat{\mathbb{F}} \cdot \delta l} \tag{12}$$

IV. Correction for Approximation Error in the Strip Plane

To illustrate the modification of the FDTD algorithm with correction factors we shall examine the H_y iteration equation that applies close to a strip edge in its plane, Fig. 2. We can assume, from half-plane theory [2], that close to the edge the field components assume the following approximate static forms:

$$H_y(x, z) \simeq Ax^{-0.5}(Bz + C) \tag{13}$$

$$E_x(x) \simeq Dx^{-0.5} \tag{14}$$

$$E_z(z) \simeq (Ez + F) \tag{15}$$

where the origin for x lies at the strip edge as shown.

We denote β as the projection of the strip edge into the cell of width δx, as illustrated in Fig. 2, and α as the ratio:

$$\alpha = \frac{\beta}{\delta x}. \tag{16}$$

By using the assumed field forms in the integral equations (11) and (12) we produce the following correction factors:

$$\mathrm{CF}_s(H_y) = \mathrm{CF}_1(E_x) = 2\sqrt{(1-\alpha)(0.5-\alpha)} \tag{17}$$

where $0 \le \alpha < 0.5$. As the transverse electric field component, E_z, is assumed linear between nodes, no significant errors are generated by it through the FDTD approximations. The correction factors can be predetermined from the geometries of the structure and the configuration of the lattice.

Hence we can apply the following augmented FDTD iteration equation for the H_y fields along the edge to remove FDTD approximation errors (c.f., (10)):

$$H_y^{t+dt} = H_y^t + \frac{\delta t}{\mu \cdot \mathrm{CF}_s}\left(\frac{(E_z^+ - E_z)}{\delta x} + \frac{(E_x - E_x^+)\mathrm{CF}_1}{\delta z}\right). \tag{18}$$

It is interesting to note that a specific value of the edge projection ratio; $\alpha = (3 - \sqrt{5})/4 \approx 0.19$, ensures that the correction factors in this instance all equal one. In other words it is possible to position the lattice so as to eliminate these FDTD approximation errors in the strip plane. It is to be noted that the value of α chosen will affect the FDTD frequency results, as it directly changes the line width/length of the structure as seen by the model and hence its effective capacitance.

Using a value for α of 0.19 when deciding on the configuration of the model mesh is a sensible choice for the above reason. However, it is not always possible to position the lattice in such a manner for more complex structures without incurring run-time penalties due to small cell sizes having to be used with a correspondingly small time step. Fig. 3 highlights the problem for a typical MMIC configuration. Furthermore, fields immediately above and below discontinuities also exhibit large spatial variation

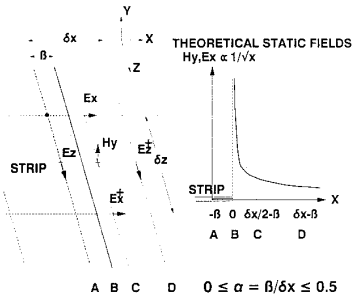

Fig. 2. *Hy* difference equation variables at a strip edge.

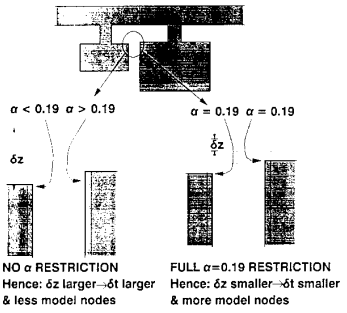

Fig. 3. Typical lattice positioning problems.

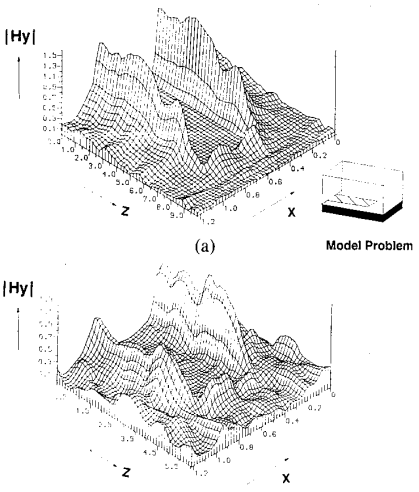

Fig. 4. Snapshots taken from the modeling of the open end discontinuity. (a) $|H_y|$ in the strip plane. (b) $|H_y|$ below the strip plane.

which will produce approximation errors that are not eliminated by using this value of α. Fig. 4 shows a snapshot of singular H_y fields arising during the modeling of an open-end using the resonance method, taken both in the plane of the strip and below it. To the authors' knowledge, no analytical solutions for the field distributions here are available. A knowledge of the behaviour of the fields in these regions is required to enable the calculation of correction factors for all the approximation errors generated from the FDTD algorithm.

V. Laplace Solution

De Smedt and Van Bladel [12], [14] formulated a method for solving the Laplace equation in spherical coordinates to give the electric and magnetic potentials existing close to the tip of a flat metallic sector of arbitrary opening angle. The technique was recently utilized by Marchetti and Rozzi [15], [16] as a means of enhancing the Transverse Resonance Diffraction Method. To solve the static problem we assume the electric potential, Φ, and the magnetic potential Ψ, to be of the form

$$\Phi(R, \theta, \phi) = R^{\nu} Y(\theta, \phi) \tag{19}$$

$$\Psi(R, \theta, \phi) = R^{\tau} Z(\theta, \phi) \tag{20}$$

The function Y is an eigenfunction of the problem:

$$\nabla^2 Y + \nu(\nu + 1) Y = 0$$

$$Y = 0 \text{ on sector.} \tag{21}$$

The functional J, which is stationary with respect to eigenfunction Y, is given in [14] by

$$J(Y) = \int_s \left[|\text{grad}_s Y|^2 - \nu(\nu + 1) Y^2 \right] dS$$

$$= \int\int \left[\left(\frac{\partial Y}{\partial \theta} \right)^2 + \frac{1}{\sin^2 \theta} \left(\frac{\partial Y}{\partial \phi} \right)^2 \right] \sin \theta \cdot d\phi \cdot d\theta - \nu(\nu + 1) \int\int Y^2 \sin \theta \cdot d\phi \cdot d\theta. \tag{22}$$

The eigensolution $Y(\theta, \phi, \theta m, \nu_{\text{low}})$ of (21), for a particular sector of opening angle $2\theta m$, corresponding to the lowest eigenvalue ν_{low} can be calculated using the finite element method, and stored in a database file. Fig. 5 shows the type of sectors most commonly seen in MMIC's, indicating that database solutions for $\theta m = \pi/2$, $\pi/4$ and $3\pi/4$ are those usually required.

We use standard finite-element procedure [17] to solve the eigen-problem, so only an overview is given for the method—The problem space, $Y(0 \le \theta \le \pi, 0 \le \phi \le \pi/2)$, is divided up into triangular elements and approximated using standard local trial functions, $\Delta^{(i)}$, as shown in Fig. 6. Typically 3500 elements are used for each solution. In minimising the functional given in (22), the elemental stiffness and mass elemental matrices are calculated, which are then combined into the global stiffness $[K_{ij}]$ and mass $[M_{ij}]$ matrices using standard finite-element techniques. These are banded, symmetrical matrices and so can be compressed to allow for a finer solution. This results in the following matrix eigenvalue problem:

$$([K_{ij}] - \nu(\nu + 1)[M_{ij}]) \cdot \xi_j = 0$$

$$Y = \sum_i \xi_i \cdot \Delta^{(i)}. \tag{23}$$

The lowest eigenvalue, ν_{low}, and its corresponding eigenvector, ξ_{low}, of problem (23) is found from a standard NAG[1] library procedure using a varient of the method of

[1]Numerical Algorithm Group, Oxford.

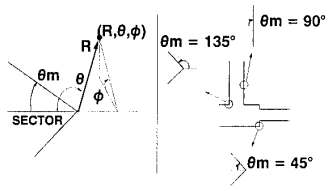

Fig. 5. Commonly seen sectors in MMIC Circuitry.

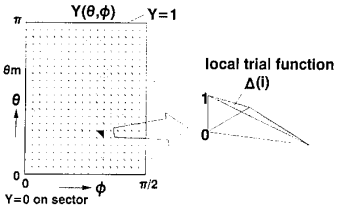

Fig. 6. Finite element solution space for Y.

Crawford [18]. The components of ξ_{low} give the discretized solution for Y, to be stored in the database file. Hence we can obtain the static form of the electric field, in rectangular coordinates, close to the metallic sector, from the grad of the electric potential, Φ, through interpolation of these database files:

$$E = \begin{pmatrix} E_x \\ E_y \\ E_z \end{pmatrix} = -(\text{grad } \Phi)_{(x,y,z)}$$

$$= \frac{-1}{R^{1-\nu}} \left\{ \nu Y \begin{pmatrix} \sin\theta \cdot \cos\phi \\ \sin\theta \cdot \sin\phi \\ -\cos\theta \end{pmatrix} + \frac{\partial Y}{\partial \theta} \begin{pmatrix} \cos\theta \cdot \cos\phi \\ \cos\theta \cdot \sin\phi \\ -\sin\theta \end{pmatrix} + \frac{1}{\sin\theta} \cdot \frac{\partial Y}{\partial \phi} \begin{pmatrix} -\sin\phi \\ \cos\phi \\ 0 \end{pmatrix} \right\}. \quad (24)$$

The zero-order magnetic potential, $\Psi(R, \theta, \phi, \theta_m)$, is easily obtained from the solution for the electric potential, Φ, with opening angle $2(\pi - \theta m)$. It is used to produce the expected magnetic field close to a sector, from the grad of Ψ. A database of electric potential solutions for commonly seen sectors in MMIC circuitry can be quickly established. Hence the theoretical electric and magnetic fields that exist around discontinuities can be produced and transformed into rectangular coordinates. Thereby, integrals of the form of (11) and (12) can be calculated through a discretization of the integral domain, which enables the calculation of correction factors for electromagnetic fields outside of the strip plane.

The application to a microstrip edge deserves special mention. The edge can be considered a sector of opening angle $\theta m = \pi/2$. We expect no transverse dependence of the static fields along the edge therefore all points in the integral region are assumed to be $\theta = 0$ or π. However, to overcome the $1/\sin\theta$ singularity that exists in equation (24), it is necessary to use a value of $\theta = \pi - \delta$, (where δ is small) in the calculation of the expected fields. A bonus of the non-transverse dependence along an edge is that the correction factors for a node near an edge are all identical with those of other nodes further along the edge. In other words it is only necessary to calculate the correction factors for an edge once.

VI. Correction Factor Implementation

To illustrate the use of correction factors in the FDTD method, we shall inspect the difference equation for E_x that applies close to a microstrip edge. This is an important source of FDTD approximation error. A summarized derivation of the E_x difference equation modified to include correction factors, (CF), is given starting from Ampere's law assuming a loss-less environment:

$$\frac{\partial}{\partial t} \int \varepsilon \boldsymbol{E} \cdot d\boldsymbol{S} = \oint \boldsymbol{H} \cdot d\boldsymbol{l} \quad (25)$$

With linear approximations in space as in (6) and (7) and time, Yee's E_x difference equation follows:

$$E_x^{t+dt} = E_x^t + \frac{\delta t}{\epsilon} \left(\frac{(H_y^- - H_y)}{\delta z} + \frac{(H_z - H_z^-)}{\delta y} \right). \quad (26)$$

If we correct for the spatial approximations as in (11) and (12), using the static forms of electric and magnetic fields obtained from the Laplace solution, we form the modified difference equation:

$$E_x^{t+dt} = E_x^t + \frac{\delta t}{\text{CF}_s \cdot \epsilon} \left(\frac{(H_y^- \cdot \text{CF}_{11} - H_y \cdot \text{CF}_{12})}{\delta z} + \frac{(H_z \cdot \text{CF}_{13} - H_z^- \cdot \text{CF}_{14})}{\delta y} \right) \quad (27)$$

Fig. 7 highlights the E_x difference equation variables that apply close to a microstrip edge. It also shows the expected E_x field in the region and the expected FDTD approximation error arising from (6) and (7) which necessitates correction. It is interesting to note that correction factor CF's in (27) has the effect of altering the effective permittivity and hence accounts for the local fringing capacitance.

This procedure can be extended to allow the formulation of modified difference equations for all the electromagnetic fields around discontinuities. The correction factors for a node will depend on its position relative to a discontinuity, and on the lattice dimensions around it. When compared with standard FDTD implementation, extra processing time is required, before iteration begins, to calculate all the correction factors for the model through

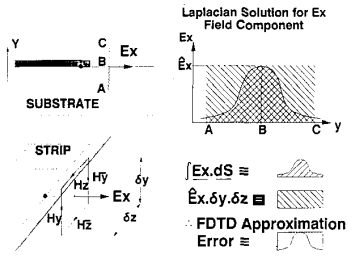

Fig. 7. *Ex* field component close to a strip edge.

evaluation of integrals arising from (11) and (12). The integrals are calculated through a discrete summation of the field values over the integral regions, which are obtained through linear interpolation of the database potential files. Accuracy is high due to the (R, θ, ϕ) dependence of the potential files, as any field singularity information is contained in the R^n term. The pre-processing time is minimal as the majority of the static field calculation is already done in the formation of the database files. A little extra time is also invested on each iteration in applying the modified difference equations at the chosen nodes close to any discontinuities.

In order to reduce storage and processing requirements for the correction factors, only those fields and nodes that are significantly affected by the discontinuity are corrected. As might be expected, it is found that greatest improvement in accuracy comes from correcting the field components containing the most energy, and from correcting the nodes closest to the discontinuity where most field variation is displayed. Overall extra processing time is found to be of the order of 1%.

VII. Results for Closed Structures

In [19], Shorthouse and Railton produced results for the microstrip line and open-end discontinuity, analyzed using the basic resonance method FDTD, the FDTD with correction factors and finally, the SDM method. The beneficial effects of using correction factors both in speed and accuracy were demonstrated. Correction factors were used in the modeling of the open-end discontinuity to demonstrate the benefits of correction factor implementation over a wide variation in α. All the open-end models in this paper use a substrate having $\epsilon_r = 9.7$ and of height 1.27 mm. Strip widths are all 1.27 mm. Fig. 8 displays the fundamental resonances obtained during the modelling of open-ends of lengths 5 mm and 8 mm. The model configurations are given in Tables I and II, respectively. Results are obtained using FDTD models having coarse meshes; with and without correction factors, and with *force majeure*, fine mesh models that take longer to run and are taken to be accurate based on previous experience. A normalized run-time figure (NRT) is used to compare run-times between different FDTD models which takes into account model nodes and model time step:

$$\text{NRT} \propto \frac{\text{Nodes}}{\text{Time Step}}. \tag{28}$$

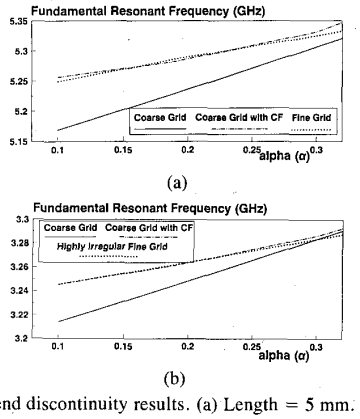

Fig. 8. Open-end discontinuity results. (a) Length = 5 mm. (b) Length = 8 mm.

The FDTD runs utilizing correction factors use the modified difference equations have correction only for selected field components close to discontinuities that are situated in the plane of the strips and immediately below them. The improvement in accuracy from this form of FDTD algorithm modification is clearly demonstrated, whereby accurate results can be obtained using coarser grids than normal. In these examples, where irregular lattices were used throughout, a reduction in run time of the order of 8 times is displayed when compared with an optimal irregular lattice. The order of time saving would be even greater if compared to the widely used regular lattices.

To demonstrate how the calculated resonant frequency may be made constant, over a wide variation in α, through the use of correction factors, the 5 mm open-end was again modeled this time only using correction in the strip plane. Fig. 9 displays the fundamental resonance obtained. The rise in calculated resonant frequency with α in the uncorrected runs is due to the fact that the effective width of the line as seen by the model becomes less. The relatively level curve for the calculated frequency response of the corrected runs indicates that the α dependencey of model prediction may be removed by correction factors which enables a more flexible approach to the positioning of the model lattice. This gives benefits both in number of model nodes and in the model time step, as indicated by Fig. 3.

VIII. Results for Open Structures

In order to demonstrate the use of correction factors on open structures using pulse excitation analysis, the low pass filter that was analyzed by Sheen *et al.* [20] using FDTD analysis and a regular lattice, was again analyzed by the FDTD method. The model geometry is given in Fig. 10. We aim to show how the speed of Sheen's analysis can be substantially improved through the use of an irregular lattice, and then further improved through the use of correction factors. Apart from the ground plane, the walls of the model had a form of Mur's [21] first order absorbing boundaries imposed on them, which have been adapted to allow for a nonuniform lattice [22]. A

TABLE I
MODEL CONFIGURATIONS USED IN THE SIMULATION OF THE MICROSTRIP OPEN-END DISCONTINUITY, LENGTH = 5 mm

FDTD Model Type: (Open-End Length = 5 mm)	Coarse Grid ——	Coarse Grid with CF - - - -	Fine Grid ----------
Nodes	20 × 12 × 20	20 × 12 × 20	40 × 24 × 20
Time Step (pS)	0.528	0.528	0.264
NRT[3] (1.00 ≡ 58.3 CPU min)	1.00	1.01	26.67

[3]Run times given for a Gould NP1 mini-computer.

TABLE II
MODEL CONFIGURATIONS USED IN THE SIMULATION OF THE MICROSTRIP OPEN-END DISCONTINUITY, LENGTH = 8 mm

FDTD Model Type: (Open-End Length = 8 mm)	Coarse Grid ——	Coarse Grid with CF - - - -	Highly Irregular Fine Grid ----------
Nodes	20 × 12 × 20	20 × 12 × 20	24 × 20 × 24
Time Step (pS)	0.729	0.729	0.364
NRT[3] (1.00 ≡ 53.6 CPU min)	1.00	1.01	8.01

[3]Run times given for a Gould NP1 mini-computer.

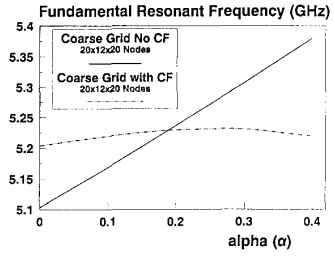

Fig. 9. Open-end discontinuity modeling with varying α.

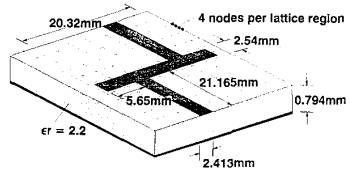

Fig. 10. Low-pass filter geometry showing lattice regions for model B.

Gaussian pulse was used as the excitation because it is smooth and has a Fourier Transform that is also Gaussian. As in the Sheen FDTD model, the time constant of the pulse was 15 pS with an overall duration of 90 pS. To ensure a pulse launch undistorted by the model boundary, the vertical components of the $\boldsymbol{E}$ fields were excited under the feed-line two nodes inside the absorbing boundary. This set up two pusles travelling in opposite directions. The receding one was absorbed by the absorbing boundary. A time history was taken at a node just below the feedline whose position was chosen so as to allow for separation of the input and reflected waves. A time history was also taken just under the output line. The vertical $\boldsymbol{E}$ field components in the time histories can be assumed proportional to the voltage on the lines, as long as the line widths are the same, and can be directly fourier transformed to produce frequency dependent S-parameters.

Table III displays the configurations of FDTD models used. We use Sheen's measured results obtained from a HP-8510 network analyser, and a Touchstone® simulation for further comparison. Fig. 11 displays the wide-band S-parameter results for the measured case, the Touchstone simulation and the best irregular lattice FDTD simulation model found, (B). The model (B) was the best found in terms of overall speed and accuracy, and is similar to the one used in [23]. The results are generally in agreement in showing the characteristic troughs, but diverge from the measured for the higher frequencies. An FDTD model will become less accurate as the frequency rises because the mesh size becomes a larger fraction of wavelength, and the higher frequency components in the initial Gaussian pulse are relatively less. Touchstone results are based on combinations of empirical formulas and quasi-static models which will be expected to reduce in accuracy with increasing frequency. It must also be noted that the HP-8510 network analyzer was only calibrated to 18 GHz, furthermore, measured results in these regions become increasingly sensitive to connector imperfections, substrate permittivity tolerances and metal etching tolerances. However, with these points in mind, it is reasonable to compare results for all methods and models by looking more closely at the S-parameter troughs.

Fig. 12 displays S21 results over 5.5 to 9 GHz for our FDTD models (B, C, D), Sheen's FDTD model (A), Sheen's measured data and the Touchstone simulation. The Touchstone simulation is quite poor here, only picking out a central trough. Sheen's regular lattice model (A),

®A registered trademark of EEsof, Inc.

TABLE III
MODEL CONFIGURATIONS USED IN THE SIMULATION OF THE LOW PASS FILTER

	FDTD Model Type: (Low Pass Filter)	Nodes	Time Step (pS)	NRT[3] (1.00 ≡ 48.5 CPU min)
A	Sheen [20] Regular Lattice	128 000	0.696[4]	8.01
B	Best Irregular Lattice	25 344	0.508	2.18
C	Coarse Irregular Lattice	12 096	0.527	1.00
D	Coarse Irregular Lattice with CF	12 096	0.527	1.01

[3]Run times given for a Gould NP1 mini-computer.
[4]Using the same stability criterion as for models B, C and D.

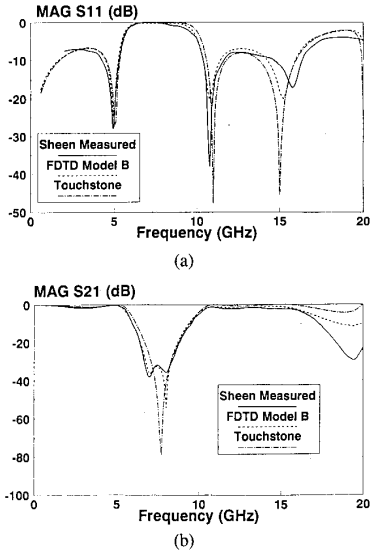

Fig. 11. Wide-band low-pass filter results. (a) $|S_{11}|$. (b) $|S_{22}|$.

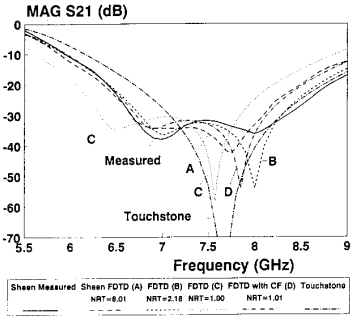

Fig. 12. Narrowband comparison of low-pass filter $S21$ results.

although taking about 3.7 times longer to run than the best irregular lattice model (B), is the further removed from the measured data. This is due to having a larger cell size around the discontinuities, and hence, the worse model definition. FDTD model C uses less nodes in a coarser lattice than model B, which allows a larger time step, (0.527 pS as opposed to 0.508 pS), and a run-time of less than half that of model B. The main trough is about 400 MHz down on the measured and model B. FDTD model D uses the same lattice as model C but uses correction

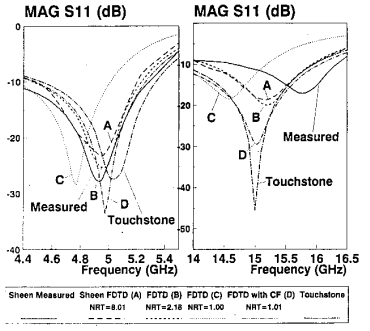

Fig. 13. Narrowband comparison of low-pass filter $S11$ results.

factors in the strip plane and just below it. The trough has been substantially shifted upwards by the use of correction factors and is now nearer to the measured than Sheen's model (A) which took approximately eight times longer to run.

Fig. 13 displays $S11$ results for the first and last troughs; over 4.4 to 5.5 GHz and over 14 to 16.5 GHz, respectively. The same conclusions as for the S21 results generally apply. The frequency shifts on the coarser models through the use of correction factors may be seen on both graphs, indicating that correction factor performance is frequency robust. For reasons explained above, it is important not to give too much credence to the higher frequency range results due to the uncertainty over the measured data.

IX. CONCLUSION

The incorporation of correction factors into the FDTD algorithm applied to the field components close to microstrip discontinuities has been shown to give a marked improvement in model accuracy for both resonator and pulse analysis. This equates to considerable savings in computer processing time, because required accuracy can be achieved using a coarser lattice which means less nodes and a larger time step in the model. Correction factors have also been shown to produce a level frequency response over a wide range of α variation. This enables much greater freedom in the placement of the model lattice which again allows fewer nodes and a larger model time step. With the use of irregular lattices, the order of time saving indicates that FDTD analysis of complex

MMIC circuitry is now feasible on moderate power computers.

The technique should be especially effective wherever brute force lattices have to be used to give adequate definition to finely detailed structures, thin lines or gaps. In MMIC's, curved structures are in fact composed of short line segments, (e.g. a circle being typically 32 sided). The new technique allows for correction of corners of arbitrary angle so that the effects of curves and beveled corners can be predicted without staircasing approximation errors.

ACKNOWLEDGMENT

The authors would like to thank the U.K. Science and Engineering Research Council and GEC-Marconi Materials Research (Caswell) for the provision of a case award and financial support.

REFERENCES

[1] K. S. Yee, "Numerical solution of initial boundary value problems involving Maxwell's equations in isotropic media," *IEEE Trans. Antennas Propagat.*, vol. AP-14, no. 3, pp. 302–307, May 1956.

[2] A. Taflove and K. Umashankar, "Radar cross-section of general three dimensional scatterers," *IEEE Trans. Electromagn. Compat.*, vol. EMC-25, pp. 433–440, Nov. 1983.

[3] C. J. Railton and J. P. McGeehan, "Analysis of microstrip discontinuities using the finite difference time domain technique," in *IEEE MTT-S Int. Microwave Symp. Dig.*, Long Beach, CA, June 1989, pp. 1009–1012.

[4] R. H. Jansen, "The spectral-domain approach for microwave integrated circuits," *IEEE Trans. Microwave Theory Tech.*, vol. MTT-33, pp. 1043–1056, Oct. 1985.

[5] C. J. Railton and J. P. McGeehan, "An analysis of microstrip with rectangular and trapezoidal conductor cross sections," *IEEE Trans. Microwave Theory Tech.*, vol. MTT-38, no. 8, pp. 1017–1022, Aug. 1990.

[6] N. M. Pothecary and C. J. Railton, "Analysis of cross-talk on high speed digital circuits using the finite difference time domain method," *Int. J. Numerical Modelling*, vol. 4, pp. 225–240, Sept. 1991.

[7] A. Taflove and M. E. Brodwin, "Numerical solution of steady-state electromagnetic scattering problems using the time-dependent Maxwell's equations," *IEEE Trans. Microwave Theory Tech.*, vol. MTT-23, pp. 623–630, Aug. 1975.

[8] D. H. Choi and W. J. R. Hoefer, "The finite-difference-time-domain method and its application to eigenvalue problems," *IEEE Trans. Microwave Theory Tech.*, vol. MTT-34, pp. 1464–1469, Dec. 1986.

[9] R. H. Jansen and Ing, "Hybrid mode analysis of end effects of planar microwave and millimetrewave transmission lines," *Proc. Inst. Elec. Eng.*, vol. 128, pt. H, no. 2, Apr. 1981.

[10] A. Reineix and B. Jecko, "Analysis of microstrip patch antennas using finite difference time domain method," *IEEE Trans. Antennas Propagat.*, vol. AP-37, no. 11, pp. 1361–1369, Nov. 1989.

[11] X. Zhang and K. K. Mei, "TD-FD approach to the calculation of the frequency-dependant characteristics of microstrip discontinuities," *IEEE Trans. Microwave Theory Tech.*, vol. 36, no. 12, pp. 1775–1787, Dec. 1988.

[12] R. De Smedt and J. G. Van Bladel, "Field singularities near aperture corners," *Proc. Inst. Elec. Eng.*, vol. 134, pt. A, pp. 694–698, Sept. 1987.

[13] A. Taflove, K. R. Umashankar, B. Beker, F. Harfoush, and K. S. Yee, "Detailed FD-TD analysis of electromagnetic fields penetrating narrow slots and lapped joints in thick conducting screens," *IEEE Trans. Antennas Propagat.*, vol. 36, pp. 247–257, Feb. 1988.

[14] R. De Smedt and J. G. Van Bladel, "Field singularities at the tip of a metallic cone of arbitrary cross section," *IEEE Trans. Antennas Propagat.*, vol. AP-34, pp. 865–870, July 1986.

[15] S. Marchetti and T. Rozzi, "Electric field singularities in microwave integrated circuits (MIC)," in *Proc. 20th European Microwave Conf.*, Budapest, Sept. 1990, pp. 823–828.

[16] S. Marchetti and T. Rozzi, "Electric field behavior near metallic wedges," *IEEE Trans. Antennas Propagat.*, vol. AP-38, no. 9, pp. 1333–1340, Sept. 1990.

[17] G. String and G. J. Fix, *An Analysis of the Finite Element Method.* Englewood Cliffs, NJ: Prentice-Hall, 1973.

[18] C. R. Crawford, "Reduction of a band-symmetric generalized eigenvalue problem," *Comm. ACM*, no. 16, pp. 41–44, 1973.

[19] D. B. Shorthouse and C. J. Railton, "Incorporation of static singularities into the finite difference time domain technique with application to microstrip structures," in *Proc. 20th European Microwave Conf.*, Budapest, Sept. 1990, pp. 531–536.

[20] D. M. Sheen, S. M. Ali, M. D. Abouzahra, and J. A. Kong, "Application of the three dimensional finite-difference time domain method to the analysis of planar microstrip circuits," *IEEE Trans. Microwave Theory Tech.*, vol. 38, no. 7, pp. 849–857, July 1990.

[21] G. Mur, "Absorbing boundary conditions for the finite-difference approximation of the time-domain electromagnetic-field equations," *IEEE Trans. Electromagn. Compat.*, vol. EMC-23, no. 4, pp. 377–382, Nov. 1982.

[22] E. M. Daniel and C. J. Railton, "An improved second order radiating boundary condition for use with non-uniform grids in the finite difference time domain method," in *Proc. 21st European Microwave Conf.*, Stuttgart, Sept. 1991, pp. 547–552.

[23] D. L. Paul, E. M. Daniel, and C. J. Railton, "A fast finite difference time domain method for the analysis of a planar microstrip filter," in *Proc. 21st European Microwave Conf.* Stuttgart, Sept. 1991, pp. 199–204.

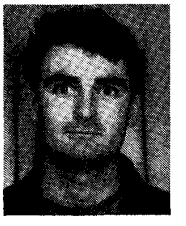

David Shorthouse was born in Nuneaton, England in 1965. He received the B.Sc. degree in engineering mathematics from the University of Bristol, England in 1988. He is in the process of completing his thesis for the Ph.D. degree in electrical engineering, the work for which has been undertaken at the Centre for Communications Research (CCR), University of Bristol. The research has involved investigating techniques for increasing the efficiency of the Finite Difference Time Domain technique for particular application in analysis of passive microwave structures.

He is currently employed at the CCR where he is investigating infrared propagation in the home environment.

C. J. Railton (M'88), for a photograph and biography, see this issue, p. 985.